The Egyptian Journal of Radiology and Nuclear Medicine (2012) 43, 623–630

Egyptian Society of Radiology and Nuclear Medicine

The Egyptian Journal of Radiology and Nuclear Medicine

www.elsevier.com/locate/ejrnm
www.sciencedirect.com

ORIGINAL ARTICLE

Assessment of ureteric obstruction with 16-MDCT: Curved planar reformats versus three-dimensional volume-rendered images and their corresponding maximum intensity projections

Mohamed Shweel [a,*], Enas A. Abd-El Gawad [a], Ehab A. Abd-El Gawad [a], Tarek K. Fath El Bab [b]

[a] *Department of Radiology, Minia University Hospital, Al-Minia, Egypt*
[b] *Department of Urology, Minia University Hospital, Al-Minia, Egypt*

Received 24 June 2012; accepted 20 September 2012
Available online 16 October 2012

KEYWORDS

Mutidetector CT urography;
Postprocessing techniques;
Ureteral obstruction

Abstract *Aim:* To compare the sensitivity and diagnostic accuracy of curved planar reformation (CPR) image on the one hand versus combined volume-rendered (VR) image and its corresponding maximum intensity projection (MIP) image on the other hand for determination of the cause and level of ureteral obstruction.

Materials and methods: The study included 60 patients with clinical and sonographic manifestations of ureteral obstruction who underwent two-phase multidetector CT urography (MDCTU) using a 16-slice machine. A total of 82 ureters were examined. CPR images were performed to display the entire course of ureters in the same image. 3D VR reformats and their corresponding MIP were used to enhance visualization of opacified ureters. The sensitivity and accuracy of CPR, and combined 3D VR and MIP for diagnosis of ureteral obstruction were calculated and compared in reference to the gold standard.

Abbreviations: MDCTU, multidetector CT urography; CPR, curved planar reformation; 3D VR, three-dimensional volume-rendered; MIP, maximum intensity projection.

* Corresponding author. Address: Department of Radiology, Minia University, Kornish El Nile, Minia 6111, Egypt. Tel.: +20 862342505/1118009394.
E-mail address: mohshweel@yahoo.com (M. Shweel).

Peer review under responsibility of Egyptian Society of Radiology and Nuclear Medicine.

ELSEVIER Production and hosting by Elsevier

 http://dx.doi.org/10.1016/j.ejrnm.2012.09.006

Results: The cause of ureteral obstruction was calculous in 28/82 ureters (34.14%), and noncalculous in 50/82 (61%). The lower third ureter was the most affected level in 48/82 ureters (58.5%). The total sensitivity and accuracy of CPR for the cause of the ureteric obstruction (97.5% and 95.3%, respectively) were higher than those of 3D VR and its corresponding MIP (75% and 73.2%, respectively). CPR also was more sensitive and accurate (total sensitivity of 100% and accuracy of 100%) compared with those of combined 3D VR and its corresponding MIP (79.5% and 75.9%, respectively) for the level of ureteral obstruction.

Conclusions: CPR had superior diagnostic accuracy than 3D VR and MIP in detecting the cause and level of ureteral obstruction.

1. Introduction

Ureteric obstruction is defined as the blockage of any part of the ureter causing obstruction of urine flow from the kidney to the urinary bladder (1). It can be classified into congenital and acquired, intraluminal or extraluminal (2,3). Many imaging modalities are used to evaluate the obstructive uropathy each with its own benefits and limitations (4). Technologic advances in both computed tomography (CT) and magnetic resonance (MR) imaging have resulted in the ability to image the urinary tract in ways that surpass the intravenous urogram (5).

With the introduction of multidetector technology, multidetector CT urography (MDCTU) has become the test of choice for many urologic problems (5). The main advantage of multidetector CT urography (MDCTU) is its ability to provide a detailed anatomic depiction of each portion of the urinary tract (6). It also offers several advantages for imaging of the obstructive uropathy including: single breath-hold coverage of the entire urinary tract and rapid imaging with optimum contrast medium opacification (7–9).

By using MDCT, it is possible to employ different postprocessing techniques in addition to source axial images. Multiplanar reformation (MPR), curved planar reformations (CPR), maximum intensity projections (MIP), volume-rendering technique (VRT), and shaded surface displays (SSD) are currently the most frequently used (10). MPR is the most commonly used post processing technique, however its limitation is that visualized structures must be on the same plane. CPR provides the most useful luminal assessment and improves the visualization of tortuous anatomy. High-density structures, such as contrast-filled vessels and the collecting system, are demonstrated nicely in maximum intensity projection (MIP) images. Volume-rendered technique (VRT) is an excellent 3D technique that provides a summary picture for the referring physician (10–13).

A deeper knowledge of the potential of postprocessing techniques and their application will allow optimization of the MDCTU. The aim of our study was to compare the sensitivity and diagnostic accuracy of CPR on one hand versus combined VRT and MIP on the other hand for determination of the cause and level of ureteral obstruction.

2. Patients and methods

2.1. Patient population

This prospective study was approved by the local research ethics committee of our institution. During the period between March 2011 and April 2012, 60 consecutive patients (38 males and 22 females, age range, 38–64 years; mean age, 45.3 years ± 14.8[SD]), were referred from Urology Clinic with a diagnosis of un-explained ureteral obstruction based on ultrasound and plain radiography findings. In particular, the main reason for referral to MDCTU is a sonography examination that showed a hydronephrosis with no sufficient information about the cause and level of ureteral obstruction. Patients were referred for MDCTU as a part of investigatory work up. Exclusion criteria for the study consisted of contraindications to iodinated contrast media, such as a known allergy to iodinated contrast material, or elevated renal function tests (serum creatinine level > 1.5 mg/dL).

2.2. MDCTU technique

MDCTU examinations were performed for all patients using a 16-detector CT scanner (BrightSpeed 16; GE Medical Systems, GE Healthcare-America: Milwaukee, USA). The acquisition parameters were 120 kVp, 350 mAs, a helical pitch of 1.375:1, 0.6-s scan time, 16 × 0.625 mm detector configuration, 18.4-s total exposure time, 0.625 mm helical slice thickness, and 0.625 mm reconstruction interval with a large FOV. Patients were prepared by giving 500–750 mL of water over a 15- to 20-min period before the start of a renal CT examination.

Phases of MDCTU: two phase MDCTU (pre-contrast and delayed excretory phased) was performed for all patients. First phase, pre-contrast imaging of the abdomen extended from the dome of the liver to the symphysis pubis. An average amount of 80–100 mL of nonionic contrast material, iohexol (Omnipaque, 300 mg iodine/mL) was used at a rate of 3 mL per second using a power injector (Medrad, Stellant) via an 18-gauge catheter placed in the antecubital vein followed by 100 mL of saline infusion at the same rate. Oral contrast was not given for better detection of ureteral stones, and to facilitate MIP and 3D reformations of the contrast-filled ureters. Second phase (delayed or excretory phase) was obtained 10 min after contrast media administration and extended from the copula of the diaphragm to the symphysis pubis.

Image reconstruction and postprocessing techniques*:* the axial source images with a 0.625-mm slice were transferred to an Advantage Workstation (AW) Volume Share 2 (GE Healthcare). Curved planar reformatted (CPR) images were performed to display the entire length of ureters in the same image. It was obtained manually by drawing a line over the course of the ureter. Three-dimensional (3D) volume-rendered technique and Maximum Intensity Projection (MIP) was performed to display contrast-filled collecting systems and ureters. Editing techniques (auto-bone removal) were also used with both these post-processing techniques in certain cases to remove the bony structures overlying the ureters for better visualization and desired orientation.

2.3. Image analysis

The pre-contrast and postprocessing images (CPR, VR and its corresponding MIP) were reviewed for detection of the cause and level of ureteral obstruction. Two radiologists interpreted the images independently (observer 1, and 2). Both observers were blinded to the patient history and clinical information. Observers did not have access to the source images.

2.4. Statistical analysis

The interobserver agreement was evaluated in CPR on the one hand and combined CPR and its corresponding MIP on the other hand using the kappa statistics; a kappa value of less than 0.01–0.20 was considered as slight agreement, 0.21–0.40, fair agreement, 0.41–0.60, moderate agreement, 0.61–0.80, substantial agreement, and 0.81–0.99 almost perfect agreement. The gold standard for the diagnosis of the cause and level of ureteral obstruction in our study cohort included final reports of ureteroscopy, open surgery and pathological examination. The sensitivity, specificity and overall accuracy of CPR and combined CPR and its corresponding MIP in the diagnosis of the cause and level of ureteral obstruction were calculated in comparison with the gold standard. Data entry was done by SPSS version 13 and analyzed by the same software.

3. Results

This study included 60 consecutive patients (38 males, 22 females), age range was from 38–64 years (mean age was 45 years). The most common clinical presentation of ureteric obstruction was acute loin pain representing 60%. The clinical data and relevant patient's past history are listed in Table 1.

A total of 82 ureters were examined (38 unilateral, 18 bilateral, double right ureter in two patients and double left ureter in two patients). A total of eight causes of obstruction were identified in our study. The most common cause was ureteric stricture representing 30/82 (36.5%), followed by ureteric stones representing 28/82(34.14%). The lower third was the most affected in our study, it was encountered in 48/82 ureters (58.5%). The cause and level of ureteral obstruction as detected by MDCTU are listed in Tables 2 and 3.

Interobserver agreement was generally higher with CPR than VR and its corresponding MIP in detecting the cause of ureteric obstruction, it was perfect ($k = 0.832$) for CPR and good for VR and its corresponding MIP ($k = 0.773$). For detection of the obstruction level interobserver agreement was perfect for CPR ($K = 1$) and it was substantial for VR and its corresponding MIP ($k = 0.831$). Regarding the cause of ureteric obstruction, interobserver agreement using both postprocessing techniques was perfect ($k = 1$) in detecting ureteric stones, and stricture. It was slight ($k = 0.2$) in detecting the cause of ureteric compression using VR and its corresponding MIP. Results are detailed in Tables 4 and 5.

According to the final ureteroscopy, surgical and pathological reports, the sensitivity and accuracy of CPR on the one hand and combined VR and its corresponding MIP on the other hand were variable in detecting the cause and level of ureteric obstruction. CPR was more sensitive and accurate than combined VR and its corresponding MIP for detecting the cause and level of ureteric obstruction. The total sensitivity and accuracy of CPR for detecting the cause of ureteral obstruction were 97.5% and 95.3%, respectively. They were higher than those of the combined VR and its corresponding MIP (75% and 73.2%, respectively) ($p = 0.03$). Regarding detection of the ureteral obstruction level, CPR was more sensitive and accurate (sensitivity of 100% and accuracy of 100%) compared with the combined VR and its corresponding MIP (sensitivity 79.5% and accuracy 75.9%) ($p = 0.05$). Results are listed in Tables 6 and 7. Figs. 1–5.

Table 1 Clinical data and past history of the studied group ($n = 58$).

Presenting renal symptoms	No. of patients	Percent (%)
Loin Pain:	40/60	66.6
Acute	24/40	60
Chronic	16/40	40
Hematuria	14/60	23.3
Dysuria	6/60	10
History of:		
Bilharziasis	26/60	43.3
Urinary tract operation	8/60	13.3
Stone passing	12/60	20
Previous cesarean section	4/60	6.6

Table 2 Causes of ureteric obstruction as detected by MDCTU ($n = 82$ ureter).

Causes	NO (ureters)	Percent (%)
Ureteric stones	28	34.14
Ureteric stricture	30	36.5
Ureteric compression	8	9.75
UB masses involving ureteric orifice	4	4.87
PUJ	4	4.87
Ureteric mass	4	4.87
Ureterocele	2	2.43
Ectopic ureter	2	2.43
Total	82	100

Table 3 Level of ureteric obstruction as detected by MDCTU ($n = 82$ ureter).

Level	No (ureters)	Percent (%)
PUJ	4	4.87
Upper ureter	4	4.87
Middle ureter	16	19.51
Lower ureter	48	58.5
Ureteric orifice	10	21.19
Total	82	100

Table 4 Causes of ureteral obstruction according to observers and postprocessing technique ($n = 82$).

	Observer 1		Observer 2	
	CPR	VR and its corresponding MIP	CPR	VR and its corresponding MIP
Ureteric stones	24/28	18/28	22/28	16/28
Ureteric strictures	30/30	30/30	30/30	30/30
UB masses involving ureteric orifice	4/4	2/4	4/4	0/4
PUJ	4/4	4/4	4/4	4/4
Ureteric mass	4/4	0/4	2/4	0/4
Ureteric compression	4/8	0/8	4/8	0/8
Ureterocele	2/2	2/2	2/2	2/2
Ectopic ureter	2/2	2/2	2/2	2/2
Total	74/82	58/82	70/82	54/82

Table 5 Level of ureteral obstruction according to observers and postprocessing technique ($n = 82$).

	Observer 1		Observer 2	
	CPR	VR and its corresponding MIP	CPR	VR and its corresponding MIP
PUJ	4/4	4/4	4/4	4/4
Upper ureter	4/4	2/4	4/4	2/4
Middle ureter	16/16	14/16	14/16	14/16
Lower ureter	48/48	42/48	48/48	40/48
Ureteric orifice	10/10	6/10	8/10	4/10
Total	82/82	56/82	78/82	56/82

Table 6 Total sensitivity and accuracy of CPR, and combined VR and its corresponding MIP in detecting the cause of ureteral obstruction ($n = 82$).

Cause	Sensitivity (%)	PPV (%)	Accuracy (%)	*P* value
CPR	97.5	97.5	95.3	0.03
3D and MIP	75	95.3	73.2	

Table 7 Total sensitivity and accuracy of CPR, MIP 3D VR in detecting varying levels of ureteric obstruction ($n = 82$).

Level	Sensitivity (%)	PPV (%)	Accuracy (%)	*P* value
CPR	100	100	100	0.05
3D and MIP	86.3	92.8	83.9	

4. Discussion

Ureteric obstruction is a common cause of renal failure. A wide variety of pathological processes, intrinsic and extrinsic to the ureter, can cause obstruction. Early recognition and treatment of ureteric obstruction are the keys to preventing renal loss (1).

Intravenous urography (IVU) and ultrasound, which until now have been used as the first step in evaluating urinary tract, have limitations such as a low sensitivity for small lesion detection, and in examining patients with none or poor excretory kidney function. Recent advances in CT including software developments have led to the use of three dimensional (3D) imaging reconstruction techniques to be widely used (14–16).

Hypertension, followed by obstructive uropathy, is the most common leading cause of ESRD among Egyptian patients (17). Schistosomiasis is considered a common cause of renal failure in Egypt, most of which is due to obstructive uropathy (18). The prevalence rate of ESRD in El-Minia Governorate is increasing as it was 250 per million populations (pmp) in 2002 to 260 pmp in 2005 to 308 pmp in 2006, eventually it became 367 pmp in 2007 (19).

On the background of the present study target, we performed a two-phase MDCTU technique, first phase was pre-contrast and the second was excretory phase, we have not conducted a nephrographic phase. Such protocol added advantages, including reducing both examination length and patient's exposure to radiation. This was in line with Maher et al., (9) who stated that three-phase protocols have disadvantages including: a very high radiation dose, time consuming with a significant impact on increasing radiological daily workloads and it increases the number of images for review by the radiologist. We performed pre-contrast phase imaging of the abdomen to locate the kidneys and detect calcifications and urolithiasis. Smith et al., (20) reported that non contrast CT has 97% sensitivity and 96% specificity for the detection of renal calculi. Excretory phase was obtained 10 min after contrast media administration to evaluate the renal collecting system and ureters. Norozian et al., (16) reported that excretory phase was used to enhance the renal parenchymal and visualize the collecting system and ureters.

Various reconstruction techniques can be used for MDCT urography: including maximum intensity projection (MIP); curved multiplanar reformation (CMPR); volume rendering (VR) and virtual endoscopy. In the present study we per-

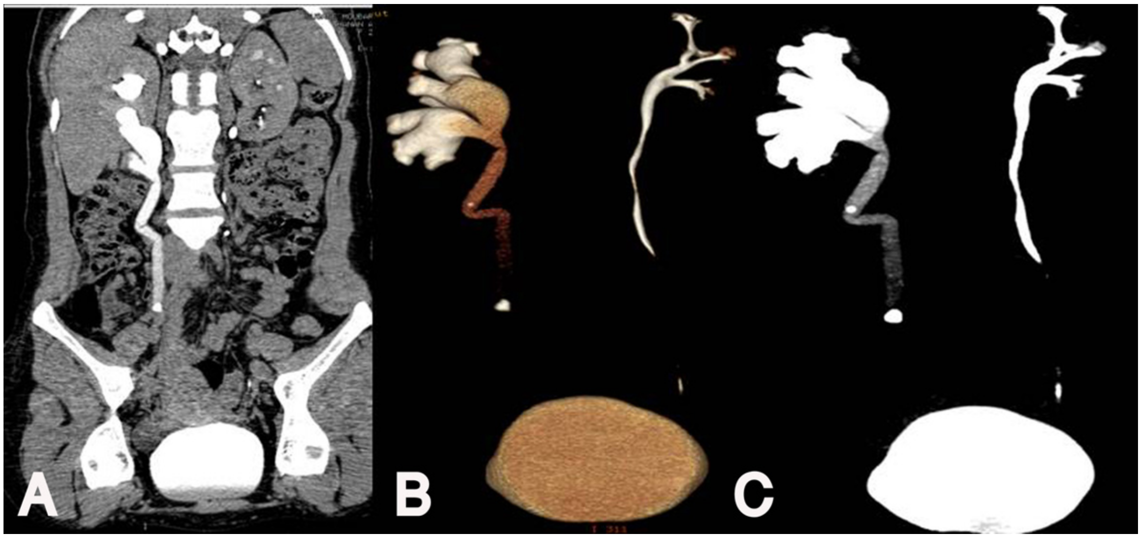

Fig. 1 Fifty-four year old patient with right hydronephrosis. Coronal CPR image (A), coronal VR (B) and its corresponding MIP (C) images in excretory phase of CT urography show clearly the cause and level of obstruction (a stone at the middle third of the right ureter). Normal left kidney and ureter. A non obstructing stone seen at the upper third right ureter.

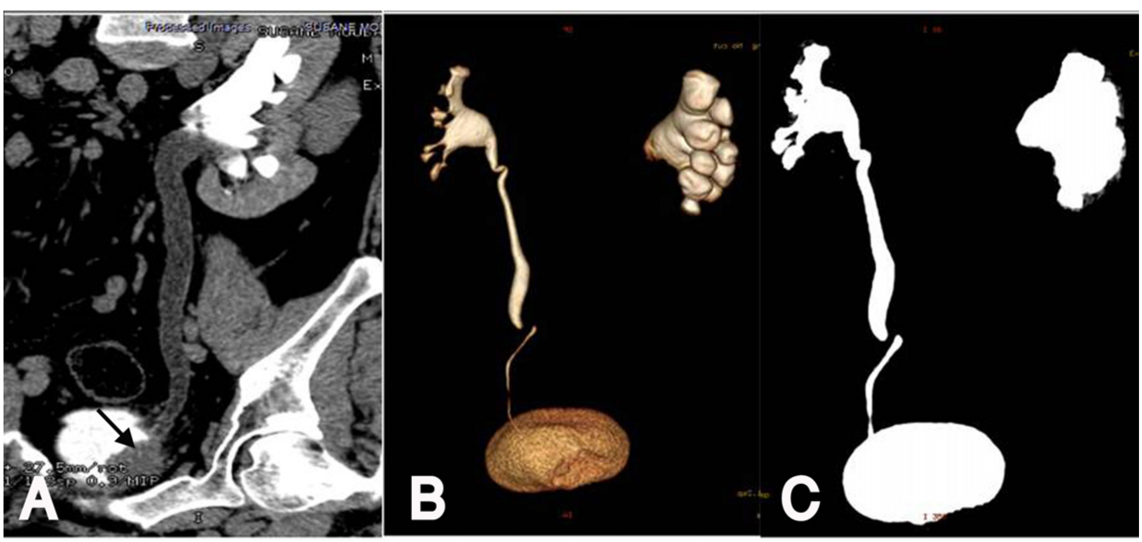

Fig. 2 Sixty-five year old male presented with hematuria. Coronal CPR (A) in excretory phase shows left hydroureteronephrosis with a UB mass obstructing the left ureteric orifice (black arrow). Reconstructed coronal VR (B) and its corresponding MIP (C) images in excretory phase of CT urography failed to delineate the cause and level of ureteral obstruction as the dilated left ureter was not seen, also the UB mass was obscured by the high density contrast in the UB.

formed CPR, 3D-VRT and its corresponding MIP, this was based on Kocakoc et al., 2005 (21) CT urography protocol that routinely used these postprocessing techniques to assess the acquired axial data.

In the present study, curved planar reformatted images were used to display the entire course of the dilated ureters in a single longitudinal uninterrupted image and hence better intraluminal and extraluminal assessment and accurate detection of the level of obstruction. Cademartiri et al., (22) stated that the most important advantage of this technique is visualization of both opacified and unopacified ureters. He postulated that CPR images could be obtained manually by drawing a line over a structure of interest or it can be produced automatically by dedicated software. In this study curved planar reformatted images were obtained only manually by drawing a line over the dilated ureters.

In our study 3D reconstruction and its corresponding MIP were obtained to clearly visualize opacified ureters and provide a roadmap for the collecting system, ureters and UB. Caoili et al., (23) reported that 3D reconstructions are a useful aid to radiologists and urologists as a ‘‘bridge’’ between excretory urography data and transverse MDCTU data. We use 3D VR reconstruction and its corresponding MIP with bone removal to display the high density ureters only without the

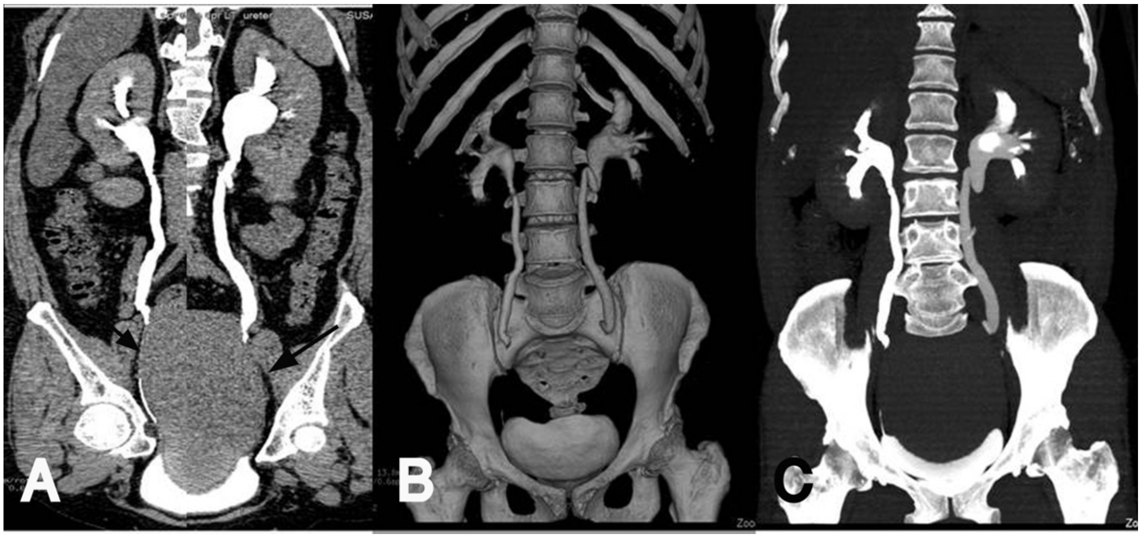

Fig. 3 Forty-three year old female presented with bilateral renal obstruction. Coronal CPR (A) in the excretory phase of CT urography clearly shows the cause and level of the obstruction which in this case a large uterine fibroid (black arrows). Reconstructed coronal VR (B) and its corresponding MIP(C) images in excretory phase of CT urography show only the level of the obstruction, while the cause was not detected.

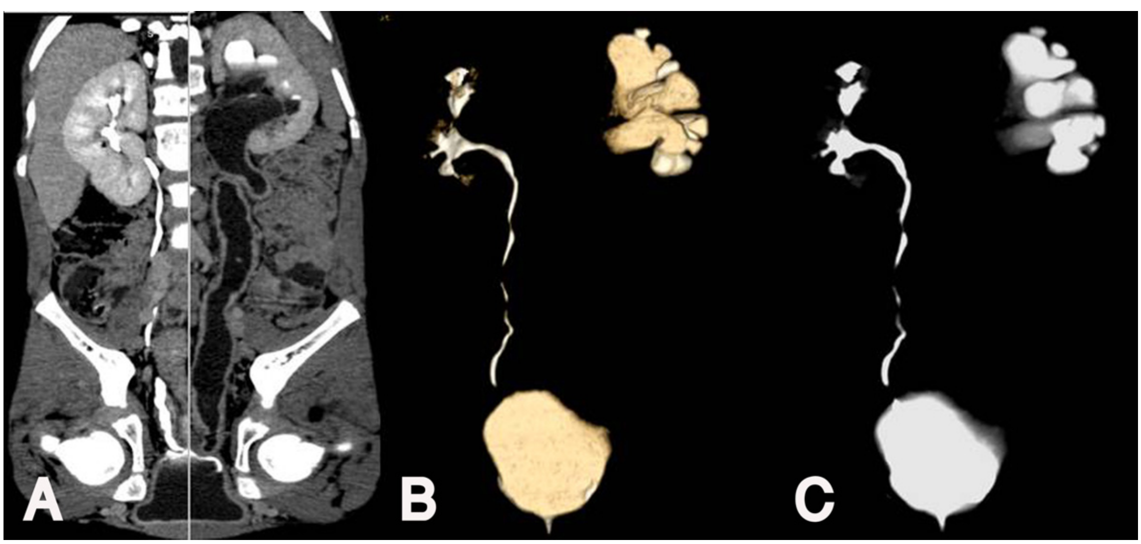

Fig. 4 Sixty-seven year old male with left loin pain. CPR at the excretory phase (A) shows delayed excretion of the left kidney, markedly dilated tortuous non opacified left ureter till its lower end with diffuse mural thickening (Bilharzial changes). Reconstructed coronal VR (B) and its corresponding MIP(C) images in the excretory phase of CT urography failed to delineate the cause and level of ureteral obstruction as the dilated left ureter was not seen.

bony structures that may obscure the course of the ureter especially its lower third that can be masked by the dense pelvic bones.

In our study the most common cause of ureteric obstruction was the ureteral stone which represented 34.14% of all cases. This was in agreement with Chevalier et al., and Shokeir et al., (24,25) who reported that ureteral obstruction is usually a consequence of nephrolithiasis which is the most common cause of urinary obstruction. The incidence of ureteral stones in this study was higher than the current data on the occurrence of urinary stones that range between 2% and 20% (26), this can be explained by that 44.82% of our patients had a previous history of bilharziasis, a common association of bilharziasis and stones was addressed by Shokeir et al., and Ghoneim et al., (25,27) who reported that urinary stasis in dilated atonic ureter invites secondary bacterial infection and stone formation. The second most common cause of obstructive uropathy in our study was the ureteric stricture with an incidence of 31.7%, this can be attributed to the high incidence of bilharziasis (44.82%). In Egypt; the prevalence of Schistosomiasis haematobium in endemic areas in Egypt ranged from 4.8% to 13.7% and averaged 7.8% (28). Ghoneim et al., (27) postulated that bilharzial ureteritis healed with variable degrees of mural fibrosis with loss of muscle and

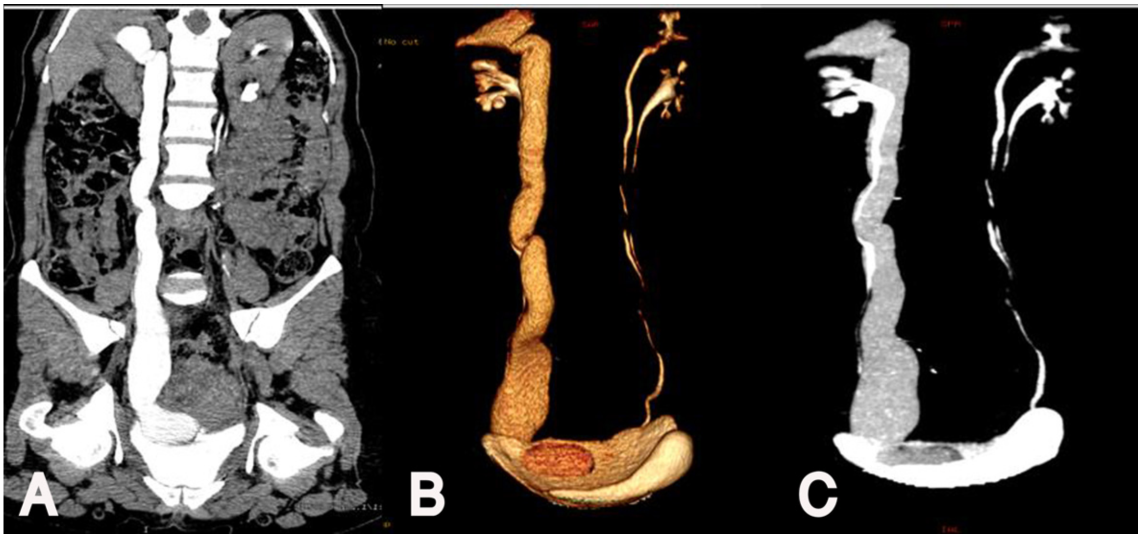

Fig. 5 Thirty-seven year old female with right loin pain. Coronal CPR image (A), reconstructed coronal VR (B) and its corresponding MIP(C) images in the excretory phase of CT urography show clearly the cause and level of obstruction. Dilated upper moiety ureter and its distal intramural dilatation (ureterocele) giving the characteristic (Copra head) appearance.

peri-ureteric adhesions that lead to ureteric stricture. In the current study, the lower third ureter was the most common level of obstruction (53.65%), this was in agreement with several authors who reported that the main site of bilharzial strictures occurred in the lower third of the ureter (28–30).

In the present study, regarding cause of ureteral obstruction, interobserver agreement was perfect in detecting ureteric stones ($k = 1$) in all postprocessing techniques (CPR, 3D VR and its corresponding MIP). This was coincided with Kocakoc et al., (21) now reported that CPR are useful in demonstrating the exact location of stones and their relationship to the ureter. Interobserver agreement was slight ($K = 0.2$) using 3D VR and its corresponding MIP in detecting the cause of ureteric compression. This could be explained by the fact that the surrounding soft tissue structures are not visualized using 3D VR and its corresponding MIP. Interobserver agreement was fair in detecting small UB masses involving the ureteric orifice using 3D VR and its corresponding MIP ($K = 0.4$), this could be explained by the same fact that the high density contrast material in the UB can mask small intraluminal lesions. This was in accordance with Caoili et al., (31) who reported that the 3D reconstructions are insufficient for visualization of small urinary tract neoplasms, and CPR will be the best post processing tool in detecting such lesions.

Regarding the level of ureteral obstruction, interobserver agreement was perfect for CPR ($K = 1$) and it was substantial for 3D VR and its corresponding MIP ($k = 0.831$).

In our study, CPR exhibit a higher sensitivity and accuracy in demonstrating the cause and level of ureteric obstruction compared with MIP and 3D VR, this was statistically significant ($p = 0.03$, $p = 0.05$, respectively). The total sensitivity and accuracy of CPR for determination of the cause of the ureteric obstruction were 97.5% and 95.3%, respectively. We believe that the most important advantages of CPR existing over MIP were that it could clarify both opacified and unopacified ureters, thus it could be used in the case of severe urinary obstruction with delayed or non-excretory function, furthermore it was superior than MIP for visualization of the ureteral environment including, soft tissue and associated extraluminal pathology.

CPR could not detect the cause of obstruction in two patients (false negative) which interpreted as normal, both showed normal ureteric wall, with no thickening or evident stricture and mild backpressure changes, by ureteroscopy ureteric stricture was detected. In contrast, 3D VR and its corresponding MIP had a low sensitivity (75%) and accuracy (73.2%) in detecting the cause of ureteric obstruction, this can be explained by that we had 26 false negative cases (14 were non excretory with unopacified ureters, so the ureters could not be displayed and the cause could not be identified, four cases had ureteric compression that could not be visualized either by 3D VR or its corresponding MIP, four had UB mass with ureteric orifice involvement and four had small ureteric mass).

CPR was highly sensitive (100%) in detecting the level of ureteric obstruction with an accuracy of 100%, unfortunately this was not true for MIP and 3D VR as we had 20 false negative cases (14 were non excretory with no contrast in the obstructed ureter, so the level could not be identified, and six showed incomplete filling of the ureter). It is not surprising that their sensitivity and accuracy was low for the cause and level of ureteral obstruction detection. This was in accord with data published by Kim et al., (14) who reported that if contrast material does not adequately fill the dilated ureter in the case of severe obstruction, CPR is more helpful. Urban et al., (12) postulated that MIP technique can be obtained with rotational viewing of multiple projections, but it lacks depth of orientation.

5. Conclusion

In detecting the cause of obstruction, the sensitivity and accuracy of CPR were significantly higher than 3D VR and its corresponding MIP. In addition, the interobserver agreement for CPR was better than that for 3D VR and its corresponding MIP. The use of CPR is recommended in the evaluation of ureteral obstruction.

References

(1) Pais Jr VM, Strandhoy JW, Assimos DG. Pathophysiology of urinary tract obstruction. In: Wein AJ, Kavoussi LR, Novick AC, Partin AW, Peters CA, editors. Campbell–Walsh urology. Saunders: Elsevier; 2007.
(2) Klahr S. Obstructive nephropathy. Kidney Int 1998;54:286–300.
(3) Walsh PC, Retnik AB, Vaughan ED, Wein AJ. Campell's urology. 7th ed. Philadelphia: W.B. Saunders Company; 1998, p. 343–60.
(4) Koelliker SL, Cronan JJ. Acute urinary tract obstruction: imaging update. Urol Clin North Am 1997;24:571–82.
(5) Silverman SG, Leyendecker JR, Amis ES. What is the current role of CT urography and MR urography in the evaluation of the urinary tract? Radiology 2009;250:309–23.
(6) Ghersin E, Brook OR, Meretik S, Kaftori JK, Ofer A, Amendola MA, et al. Antegrade MDCT pyelography for the evaluation of patients with obstructed urinary tract. AJR 2004;183:1691–6.
(7) Chow LC, Sommer FG. Multidetector CT urography with abdominal compression and three-dimensional reconstruction. AJR Am J Roentgenol 2001;177:849–55.
(8) Kim JK, Ahn JH, Park T, Ahn HJ, Kim KS, Cho KS. Virtual cystoscopy of the contrast-filled bladder in patients with gross hematuria. AJR Am J Roentgenol 2002;179:763–8.
(9) Maher MM, Kalra MK, Rizzo S, Mueller PR, Saini S. Multidetector CT urography in imaging of the urinary tract in patients with hematuria. Korean J Radiol 2004;5:1–10.
(10) Rubin GD. 3-D imaging with MDCT. Eur J Radiol 2003;45: 37–41.
(11) Mortele KJ, McTavish J, Ros PR. Current techniques of computed tomography. Helical CT, multidetector CT, and 3D reconstruction. Clin Liver Dis 2002;6:29–52.
(12) Urban BA, Ratner LE, Fishman EK. Three-dimensional volume-rendered CT angiography of the renal arteries and veins: normal anatomy, variants, and clinical applications. Radiographics 2001;21:373–86.
(13) Sheth S, Fishman EK. Multi-detector row CT of the kidneys and urinary tract: techniques and applications in the diagnosis of benign diseases. Radiographics 2004;24:20–45.
(14) Kim JK, Cho KS. CT urography and virtual endoscopy: promising imaging modalities for urinary tract evaluation. BJR 2003;76:199–209.
(15) Kalra MK, Maher MM, D'Souza R, Saini S. Multidetector computed tomography technology: current status and emerging developments. J Comput Assist Tomogr 2004;28:2–6.
(16) Norozian M, Cohan RH, Caoili EM. Multislice CT urography. Br J Radiol 2004;77:S74–86.
(17) El-Gaafary M, Abou El-Fetouh A, Zaki M, Abdel-Kerim A, Hafez AS. Some epidemiological aspects of patients with end stage renal diseases. J Egypt Public Health Assoc 2000;75: 107–29.
(18) Afifi A, Karim MA. Renal replacement therapy in Egypt: first annual report of the Egyptian Society of Nephrology, 1996. East Mediterr Health J 1999;5:1023–9.
(19) El-Minshawy O. End stage renal disease in El-Minia Governorate, Egypt: data of the year 2007. Nephro-Urol Mon 2011;3:118–21.
(20) Smith RC, Rosenfield AT, Choe KA. Acute flank pain: comparison of non-contrast enhanced CT and intravenous urography. Radiology 1995;194:789–94.
(21) Kocakoc E, Bhatt S, Dogra VS. Renal multidector Row CT. Radiol Clin North Am 2005;43:1021–47.
(22) Cademartiri F, Luccichenti G, van Der Lugt A. Sixteen-row multislice computed tomography: basic concepts, protocols, and enhanced clinical applications. Semin Ultrasound CT MR 2004;25:2–16.
(23) Caoili EM, Cohan RH, Korobkin M. Urinary tract abnormalities: initial experience with multi-detector row CT urography. Radiology 2002;222:353–60.
(24) Chevalier RL, Klahr S. Therapeutic approaches in obstructive uropathy. Semin Nephrol 1998;18:652–8.
(25) Shokeir AA, El-Diasty T, Eassa W, Mosbah A, El-Ghar MA, Mansour O, et al. Diagnosis of ureteral obstruction in patients with compromised renal function the role of noninvasive imaging modalities. J Urol 2004;171(6):2303–6.
(26) Basiri A, Shakhssalim N, Khoshdel AR, Javaherforooshzadeh A, Basiri H, Radfar MH, et al. Familial relations and recurrence pattern in nephrolithiasis. New words about old subjects. Urol J 2010;7:81–6.
(27) Ghoneim MA. Bilharziasis of the genitourinary tract. BJU Int 2002;89:22–30.
(28) El-Khoby T, Galal N, Fenwick A, Barakat R, El-Hawey A, Nooman Z, et al. The epidemiology of schistosomiasis in Egypt: summary findings in nine governorates. Am J Trop Med Hyg 2000;62:88–99.
(29) Al-Shukri S, Alwan MH. Bilharzial strictures of the lower third of the ureter: a critical review of 560 strictures. Br J Urol 1983;55:477–82.
(30) Bazeed MA, Ashamalla A, Abd-Alrazek A, Ghoneim M, Badr M. Partial flap ureteroneocystostomy for bilharzial strictures of lower ureter. Urology 1982;20:237–41.
(31) Caoili EM, Cohan RH, Inampudi P, Ellis JH, Shah RB, Faerber GJ, et al. MDCT urography of upper tract urothelial neoplasms. AJR 2005;184:1873–81.